

## A SIMPLE TECHNIQUE FOR IDENTIFICATION OF ONE-DIMENSIONAL POWDER X-RAY DIFFRACTION PATTERNS FOR MIXED-LAYER ILLITE-SMECTITES AND OTHER INTERSTRATIFIED MINERALS

V. A. DRITS, T. V. VARAXINA\*, B. A. SAKHAROV, AND A. PLANÇON\*

Geological Institute, Academy of Sciences, Moscow, Russia

**Abstract**—A very simple technique is proposed for a quantitative or semiquantitative interpretation of X-ray diffraction (XRD) patterns for two-component mixed-layer structures. It is suitable for a determination of the Reichweite ( $R$ ) values and proportions of component layers from graphical simulations of basal peak positions for mixed-layer structures with definite layer types. This technique can be successfully used for illite-smectites, but the accuracy of the results obtained for other mixed-layer structures is somewhat lower. In addition to the graphical technique, simple linear relationships are proposed for the calculation of layer proportions. Such relationships can be easily obtained for any mixed-layer structure with any  $R$  and any thicknesses of interstratified layers.

Structural parameters reported in the literature for mixed-layer illite-smectites, kaolinite-smectites, etc., were used to check the reliability of the method presented. It is concluded that the technique works well and produces parameters that are in agreement with those published.

**Key Words**—Identification, Illite-smectite, Interstratification, X-ray diffraction.

### INTRODUCTION

Mixed-layer minerals are known to be abundant in clays of diverse origins. One of the most effective techniques for identification and determination of the structural characteristics of mixed-layer minerals is the comparison of experimental XRD patterns with computer-simulated patterns from definite structural models. These models are characterized by a set of definite structural parameters such as layer types, structures, compositions, thicknesses, contents and mode of distribution, and thickness distribution of coherent scattering domains. This approach requires, however, a certain level of experience and, therefore, cannot be used by all researchers. That is why another approach is widely used. Diagrams or tables constructed on the basis of diffraction patterns calculated for the models may be used to determine the proportions of interstratified layers and the type of their interstratification.

The application of tables and diagrams is limited since they are obtained for models with fixed values for parameters that are not always adequate to describe the structure of the sample under study. For example, limitations may occur because thicknesses of mica, smectite, and vermiculite layers are variable depending on their 2:1 layer composition and type of interlayer cations and may differ from the layer thicknesses used in the models (Šrodón, 1980).

In this paper, we describe a very simple technique that allows us to simulate peak positions in XRD pat-

terns for two-component mixed-layer structures, such as illite-smectites (I/S) with the Reichweite value  $R > 0$ . This approach requires no special knowledge of complex calculations to simulate basal peak positions when layer thicknesses, proportions of layers,  $w$ , and the short-range order factor,  $R$ , are assumed. From experimental  $d$  values of basal reflections for a mixed-layer structure with known layer types the contents and their distribution pattern can be determined.

This technique was described by Drits and Sakharov (1976). This book is often referred to, but its contents remain unknown for Western readers, and the proposed method has not been used. Moreover, in the early '70s there were only a few publications comparing experimental and simulated XRD patterns. Therefore, the advantages of the method could not be demonstrated with examples of XRD patterns of natural mixed-layer minerals for which a satisfactory agreement had been obtained between experimental and simulated XRD data. At present, a representative set of experimental and simulated XRD data for different mixed-layer structures is available to demonstrate the efficiency of the technique proposed.

### DESCRIPTION OF THE TECHNIQUE

Méring (1949) has shown that random two-component mixed-layer systems can be easily identified with the use of a very simple technique whose basic idea is demonstrated in Figure 1a. This figure shows 00/ nodes of reciprocal lattices corresponding to periodic structures that consist of A and B layers. If A and B layer thicknesses are  $d_A$  and  $d_B$ , respectively, then the 00/ nodes for the two reciprocal lattices will occur

\* Present address: Orleans University, 45100 Orleans-la-Source, France.

with the periods  $q_A = 1/d_A$  and  $q_B = 1/d_B$ , respectively. Mering's first principle is that basal reflections for two-component random mixed-layer structures have to be situated along the  $c^*$  axis in reciprocal space and between the most closely spaced  $00l$  nodes corresponding to periodic phyllosilicates whose layers are interstratified in the mixed-layer structure. Such domains are shown in Figure 1a by thick lines.

Mering's second principle is that basal node positions corresponding to the mixed-layer structure depend on proportions of interstratified layers and the dependence can be represented by a simple relationship. Let the distances along the  $c^*$  axis between the node corresponding to the mixed-layer structure and the nearest  $l_A q_A$  and  $l_B q_B$  nodes corresponding to two periodic components be equal to  $x$  and  $y$ , respectively. In such a case, the proportion of A layers ( $w_A$ ) in the mixed-layer structure can be determined as

$$w_A = y/(x + y) \quad (1)$$

Mering's principles explain the origin of an irrational series of basal reflections in XRD patterns for mixed-layer minerals and predict general regularities in the formation of diffraction effects from such structures. Moore and Reynolds (1989) have applied these principles in their "Q-rule" in order to describe qualitatively the breadth of the peak in relation to the other basal peaks observed in XRD patterns of mixed-layer minerals. Mering's principles, however, are not used in practice for quantitative determination of layer type proportions for two basic reasons. First, these principles refer only to structures with  $R = 0$ . Second, they are valid only if the two "interacting" nearest nodes corresponding to two periodic structures have identical or similar "weights" or structure factors.

Nevertheless, with slight modification, Mering's approach can be adapted for determining structural parameters of mixed-layer structures with  $R > 0$ . The basic principle of this modification is the following. Reynolds and Hower (1970) showed that any mixed-layer structure in which A and B layers are interstratified with a maximum possible degree of ordering (MPDO) at a given  $R > 1$  can be considered as a disordered two-component system ( $R = 0$ ) where interstratified components are not individual layers but their combinations.

Let us consider a mixed-layer structure where A and B layers are interstratified with MPDO and  $R = 1$ , that is, if  $w_A > w_B$ ,  $P_{BB} = 0$ , or if  $w_B > w_A$ ,  $P_{AA} = 0$ . At the same time, A and B layers with MPDO and  $R = 1$  can be represented as a result of a random distribution of AB layer pairs and A ( $w_A > w_B$ ) or B ( $w_B > w_A$ ) layers. Therefore, if we consider AB layer pairs as an independent structural element, all mixed-layer structures of this particular type can be represented as completely disordered systems formed by two components AB and A ( $w_A > w_B$ ), or AB and B ( $w_B > w_A$ ). Under such

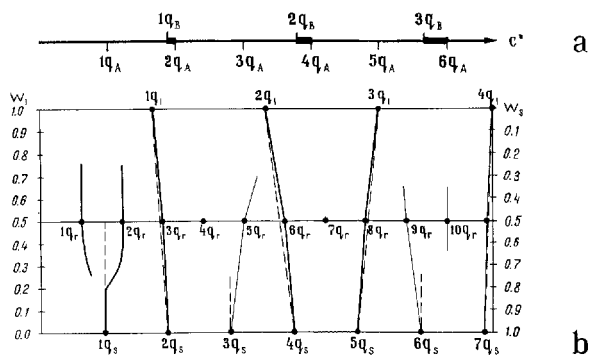


Figure 1. Graphical simulation of the distribution for nodes in reciprocal space along  $c^*$  for two-component mixed-layer structures; a) Interval between nearest reciprocal lattice nodes for two different periodic components A and B. Thick, horizontal segments indicate positions along the  $c^*$  axis where basal nodes for mixed-layer structures at  $R = 0$  have to occur (Mering, 1949). b) Node positions along  $c^*$  as a function of the value of  $w_1$  for illite-smectite mixed-layer structures saturated with glycerol and characterized  $R = 0$  (dashed lines) or by MPDO and  $R = 1$  (solid lines). Thin solid lines represent migration nodes with low-amplitude structure factors. I, illite; r, rectorite; and S, smectite.

conditions, Mering's technique can be used to characterize all mixed-layer structures with  $R = 1$ .

Additional modifications to Mering's approach consist of the following two rules (Drits and Sakharov, 1976):

- 1) If a strong reciprocal lattice node for one of the periodic components has no nearest neighbors among the reciprocal lattice nodes of the other periodic component, then it preserves its position along the  $c^*$  axis (and the corresponding basal reflection preserves its position in the XRD pattern) with decreasing proportion of the first component layers in the mixed-layer structure from 1.0 to about 0.5, but the reflection becomes less intense and broader. These effects increase rapidly at very low  $\theta$  angles. In Figure 1a,  $1q_A$  is such an isolated node.
- 2) If the  $l_1 q_1$  node of one periodic component is equidistant or nearly equidistant from the  $l_2 q_2$  and  $(l_2 + 1) q_2$  nodes of the other periodic component, then migration of the nodes for the mixed-layer structure as a function of  $w_1$  will depend on the structural amplitudes for the  $l_1 q_1$ ,  $l_2 q_2$ , and  $(l_2 + 1) q_2$  nodes. (We use here the subscripts 1 and 2 instead of A and B because not only individual layers but also layer combinations can be regarded as independent components in an interstratified structure and  $w_1$  and  $w_2$  values correspond to the proportions of these components.) If the  $l_1 q_1$  node is of low "intensity," then with  $w_2$  decreasing from 1.0 to 0.5, the behavior of  $l_2 q_2$  and  $(l_2 + 1) q_2$  will be determined by the additional rule 1.

If all three nodes are of approximately the same structural amplitude, then the number and positions

of the corresponding basal nodes of the mixed-layer structure will depend on the proportions of periodic component 1 and 2. For  $0.5 < w_1 < 1.0$ , a basal node will be observed close to the  $l_1q_1$  node. With  $w_2$  increasing from 0 to 0.5, two basal nodes of the mixed-layer structure will migrate from the positions of the  $l_2q_2$  and  $(l_2 + 1)q_2$  nodes for  $w_2 = 0$  toward the position of the  $l_1q_1$  node for  $w_1 = 0.5$ . If two nodes, e.g.,  $l_1q_1$  and  $l_2q_2$ , are substantially more intense than the  $(l_2 + 1)q_2$  node, then the migration of the mixed-layer structure node from the position of the  $l_1q_1$  node toward that of the  $l_2q_2$  node with decreasing  $w_1$  will be non-linear (curve instead of straight line) the longer the distance between the  $l_1q_1$  and  $l_2q_2$  nodes and the greater the difference between the corresponding structural amplitudes. The specific shapes of the curves representing the migration of the  $l_1q_1$  node toward  $l_2q_2$  and  $(l_2 + 1)q_2$  nodes with increasing  $w_1$  depends on the distance between the  $l_2q_2$  and  $(l_2 + 1)q_2$  nodes, the distance between  $l_1q_1$  and these nodes, and the relationship between the structural amplitudes of the three nodes involved.

The two rules provide a semiquantitative treatment for the regularities in the formation of diffraction effects from mixed-layer structures and are useful mostly for evaluating  $R$ . The validity of these rules was demonstrated by the analysis of XRD patterns simulated for various structural models (Drits and Sakharov, 1976). Application of the rules requires the knowledge of structure factors or intensities of basal reflections for periodic components whose layers or layer combinations form a mixed-layer structure. Practical use of these rules will be illustrated below.

Let us take as an example a mixed-layer structure of illite-smectite (I/S) saturated with glycerol. If we suppose, that  $d_i(001) = 10 \text{ \AA}$  and  $d_s(001) = 17.8 \text{ \AA}$ , the 00/ nodes for two reciprocal lattices will occur with the periods  $q_i = 1/10 = 0.1 \text{ \AA}^{-1}$  and  $q_s = 1/17.8 = 0.056 \text{ \AA}^{-1}$ , respectively. Figure 1b shows a rectangle whose lower side corresponds to nodes of the reciprocal lattice of smectite and the upper side contains the nodes of the illite reciprocal lattice. On the left vertical side the numbers correspond to illite contents from 1.0 at the top to 0 at the bottom with the interval of 0.1. The middle horizontal line in the rectangle drawn at  $w_1 = 0.5$  contains the nodes of the rectorite reciprocal lattice. In the rectorite structure, illite and smectite layers alternate as ISIS with period  $d_r(001) = 10 + 17.8 = 27.8 \text{ \AA}$ . Therefore, the nodes of the rectorite reciprocal lattice are distributed with period  $q_r = 1/27.8 = 0.036 \text{ \AA}^{-1}$  (Figure 1b). Let us consider the lower half of the rectangle where  $w_s > w_i$ . First of all, we have to find the pairs of nearest neighboring reciprocal lattice nodes of smectite and rectorite and join the points corresponding to every pair on the middle and lower sides of the rectangle by solid lines as is shown in Figure 1b. A peculiar mutual arrangement is observed for nodes

$1q_s$ ,  $1q_r$  and  $2q_r$ , corresponding to strong smectite 001 and rectorite 001 and 002 reflections, respectively. The distance along  $c^*$  between the  $1q_s$  and  $1q_r$  nodes is  $0.020 \text{ \AA}^{-1}$ , and the distance between  $1q_s$  and  $2q_r$  is  $0.016 \text{ \AA}^{-1}$ . Migration lines that relate these three nodes and represent the positions of basal nodes corresponding to I/S with various  $w_i$  are shown in Figure 1b, in accordance with rule 2. The structure factor for the  $4q_r$  node is close to zero, and the weak  $7q_r$  node has no nearest neighbors. As a result, the corresponding reflections will not be observed in XRD patterns.

In a similar fashion, the lines are drawn in the upper part of the rectangle in such a way that a diagrammatic representation of diffraction nodes in reciprocal space is produced that applies to all illite-smectites with MPDO of  $R = 1$  and  $w_1 > w_s$ . Note that the  $1q_r$  and  $2q_r$  reciprocal lattice nodes are now isolated, and the position of the nodes corresponding to mixed-layer I/S in this region of the reciprocal space is shown in accordance with rule 1. Diffraction nodes for every definite  $w_1$  occur at points where the horizontal line joining  $w_1$  and  $w_s = 1 - w_1$  (the right side of the rectangle) intersects the inclined solid lines connecting the reciprocal lattice nodes of periodic components.

Let us now consider the positions of diffraction maxima for I/S with  $R = 0$  using the same rectangle shown in Figure 1b. First, we shall again select pairs of nearest reciprocal lattice nodes for illite and smectite and join them as shown in the Figure 1b by dashed lines. In particular,  $1q_i-2q_s$ ,  $2q_i-4q_s$ ,  $3q_i-5q_s$  are such pairs, i.e., they always contain illite reciprocal lattice 00/ nodes. The behavior of  $1q_s$ , a strong isolated node, is shown in Figure 1b in accordance with rule 1. As noted above, the intensity and the quality of resolution of this reflection in I/S XRD patterns should decrease with increasing  $w_1$  from 0 to 0.5.

Analysis of migration lines in the rectangle shown in Figure 1b clearly shows similarities and differences in XRD patterns to be observed for I/S with  $R = 0$  and  $R = 1$  for each definite  $w_1$ . In particular, there are I/S nodes whose positions along  $c^*$  are determined by  $w_1$  and are almost independent of  $R$ . Such nodes are, e.g., those situated between  $1q_i-2q_s$ ;  $2q_i-4q_s$ ; and  $3q_i-5q_s$  node pairs for  $R = 0$  and between  $1q_i-3q_r-2q_s$ ;  $2q_i-6q_r-4q_s$ ; and  $3q_i-8q_r-5q_s$  triples for  $R = 1$  (Figure 1b). That is why reflections belonging to this group can be used to determine the proportions of layer types even in cases of mixed-layer structures without MPDO but with  $R = 1$  when  $w_1 > w_s$  and  $w_s > P_{SS} > 0$ . These reflections correspond to the I/S 001/002, 002/004 and 003/005 for a glycerol-treated sample.

The other group of I/S nodes distinguish I/S structures differing in  $R$ . In particular, XRD patterns for I/S structures with  $0.5 < w_1 < 0.8$  and  $R = 1$  will contain certain specific "rectorite-like" reflections located near the  $1q_r$ ,  $2q_r$ ,  $gq_r$  node positions (Figure 1b).

Assume now structures with MPDO,  $w_A > w_B$ ,  $P_{BB}$

= 0 and  $R = 2$  for which  $P_{AAA} = 0$ , if  $0.67 > w_A > 0.5$ . Interstratification of A and B layers in such structures can be considered as the result of total disorder in the distribution of AAB triplets and AB pairs that are considered as independent structural elements. In the case of mixed-layer minerals with  $w_A > 0.67$ , A layers and AAB triplets have to be chosen as independent components.

Let us take as an example an I/S structure with  $0.5 < w_1 < 1$  containing glycerol molecules in expandable interlayers. Figure 2a shows a rectangle whose lower horizontal side corresponds to the reciprocal lattice nodes of rectorite with  $q_r = 0.036 \text{ \AA}^{-1}$  and the upper side contains the reciprocal lattice nodes for illite. The horizontal line corresponding to I/S with  $w_1 = 0.67$  contains reciprocal lattice nodes distributed with period  $q_{IIS} = 1/(2 \times 10 + 17.8) = 0.0264 \text{ \AA}^{-1}$  that correspond to the structure with IISIS... layer type sequence. The  $lq_{IIS}$  nodes with  $l = 5, 6, 16$ , and  $17$  have structural amplitudes close to zero.

To determine the distribution along  $c^*$  for the nodes corresponding to I/S with  $R = 2$  and  $0.5 < w_1 < 0.67$ , we should join, in the lower part of the rectangle, pairs of nearest neighboring reciprocal lattice nodes located on the horizontal lines at  $w_1 = 0.5$  and  $w_1 = 0.67$  (Figure 2a) that correspond to rectorite and the periodic IISIS... structure. The lines describing the migration of the remaining nodes—such as the “isolated”  $2q_{IIS}$  node; node triples  $9q_{IIS}$ ,  $10q_{IIS}$ , and  $7q_r$ ; and  $13q_{IIS}$ ,  $14q_{IIS}$ , and  $10q_r$  nodes—were drawn, with variation in  $w_1$ , according to the rules 1 and 2. The structural amplitude values for these nodes are taken into account. The position of diffraction peaks in an XRD curve for I/S with a certain  $w_1$  is determined by the intersection of the horizontal line that joins the given  $w_1$  and  $w_s$  with the inclined solid lines connecting the reciprocal lattice nodes of the interstratified components.

In a similar fashion, lines may be drawn in the upper part of the rectangle to join the illite reciprocal lattice nodes with those for the IISIS... structure, corresponding to I/S with  $R = 2$  and  $0.67 < w_1 < 1$ . Figure 2a shows that for this type of structure, a relatively large number of “isolated”  $lq_{IIS}$  nodes with  $l = 1, 2, 3, 9, 10$ , etc., is typical, whose behavior corresponds to rule 1. In order to reveal the difference in diffraction feature for I/S having the same  $w_1$  but differing in  $R$ , migration (dashed) lines that correspond to  $R = 1$  and  $0.5 < w_1 < 1$  are drawn in the same rectangle.

Note that the solid lines that join the  $1q_1-4q_{IIS}-3q_r$ ,  $2q_1-8q_{IIS}-6q_r$ ,  $3q_1-11q_{IIS}-8q_r$ , and  $5q_1-19q_{IIS}-14q_r$  nodes corresponding to the positions of nodes for I/S with  $w_1 > 0.5$  and  $R = 2$  are straight lines. Moreover, they practically coincide with the straight lines connecting the nodes  $1q_1-3q_r$ ,  $2q_1-6q_r$ ,  $3q_1-8q_r$ , and  $5q_1-14q_r$  for I/S with  $w_1 > 0.5$  and  $R = 1$ . In other words, the positions of basal reflections corresponding to the nodes located on the lines in question depend, primarily, on

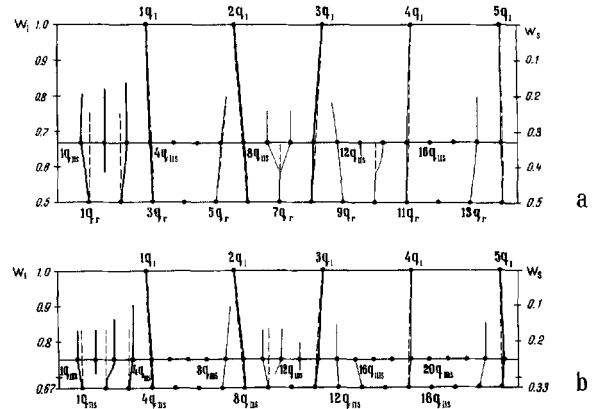


Figure 2. Graphical simulation of node positions along  $c^*$  for glycerol-containing I/S, as a function of  $w_1$ : a)  $w_1 > 0.5$ ,  $R = 1$  (dashed lines) and  $R = 2$  (solid lines); and b)  $w_1 > 0.67$ ,  $R = 2$  (dashed lines) and  $R = 3$  (solid lines). Thin solid lines represent migration nodes with low-amplitude structure factors.  $r$  = rectorite.

the proportions of the layer types but not on the order/disorder in their distribution. The remaining dashed and solid lines reveal the diffraction features that distinguish between I/S structures with  $R = 1$  and  $R = 2$  and equal  $w_1$ .

Diffraction characteristics for I/S structures with  $R = 3$  and MPDO can be determined in a similar way. Regular alternation of I and S layers with  $R = 3$  can be denoted as IISIIIS when I:S ratio is 3. The repeat distance is  $d(001) = 47.8 \text{ \AA}$  for such a structure if expandable interlayers are filled by glycerol molecules. Figure 2b shows a rectangle where a horizontal line at  $w_1 = 0.75$  contains reciprocal lattice nodes with period  $q_{IIS} = 1/47.8 = 0.0204 \text{ \AA}^{-1}$ , which is the inverse thickness of the IIS superlattice unit. The reciprocal lattice nodes of the IISIS structure ( $w_1 = 0.67$ ) are indicated on the bottom of the rectangle ( $q_{IIS} = 0.0264 \text{ \AA}^{-1}$ ) and those of illite are on the top ( $q_1 = 0.1 \text{ \AA}^{-1}$ ). Note that the  $lq_{IIS}$  nodes with  $l = 6, 7, 8, 17, 18, 20$ , and  $21$  have structural amplitudes close to zero (Figure 2b).

When  $0.75 > w_1 > 0.67$ , structures with MPDO and  $R = 3$  can be represented as resulting from random alternation of IIS and IIS superlattice units. Migration lines showing the positions of nodes along  $c^*$  for I/S structures depending on  $w_1$  are indicated in the lower part of the rectangle (Figure 2b). Structures with  $w_1 > 0.75$  can be treated as the result of random alternation of IIS superlattice units and I layers. The upper part of the rectangle in Figure 2b contains solid lines representing the migration of nodes along  $c^*$  with  $w_1$  increasing from  $0.75$  to  $1.0$ . Dashed lines in the rectangle in question correspond to migration lines that represent the nodes for an I/S structure with  $w_1 > 0.67$  and  $R = 2$ . There are again two groups of lines, one containing lines that coincide for  $R = 2$  and  $R = 3$ , and

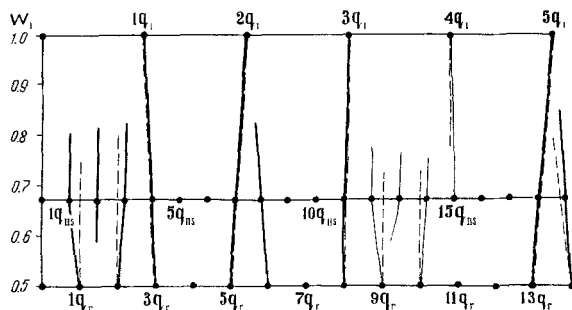


Figure 3. Graphical simulation of node positions along  $c^*$  for glycolated I/S with  $w_1 > 0.5$ ,  $R = 1$  (dashed lines), and  $R = 2$  (solid lines), as a function of  $w_1$ . Thin solid lines represent migration nodes with low structure factors.

the other with lines that distinguish between I/S differing in  $R$  and having the same  $w_1$ .

Diffraction features to be expected for glycolated I/S are similar to those revealed for glycerol-containing I/S by the graphical technique. To illustrate, let us consider the rectangle shown in Figure 3. The upper, middle, and lower horizontal sides contain reciprocal lattice nodes for illite, the IIS periodic structure, and rectorite, respectively. According to Mering's rules and rules 1 and 2, the dashed lines represent the displacement along  $c^*$  of nodes for I/S with  $R = 1$ ,  $w_1 > 0.5$  depending on  $w_1$ . Solid lines indicate the nodes for I/S with  $R = 2$ ,  $0.5 < w_1 < 0.67$  and  $0.67 < w_1 < 1$ . Again, there are two groups of nodes. In the first group, node positions depend only on  $w_1$ , while in second group, node positions are affected by order/disorder in the distribution of layer types. As a result, XRD patterns for any irregular two-component interstratified system contain two sets of reflections, the positions of which are sensitive either to 1) the proportions of layer types, or 2) to order/disorder in the distribution of layer types. Figures 1–3 show that, for I/S minerals, the second group in particular, contain reflections located in the low-angle region, i.e., reflections that correspond to reciprocal lattice nodes with  $q = 1/d_{\text{obs}} < 0.1 \text{ \AA}^{-1}$ . For example, an increase in  $R$  from 0 to 3 should be accompanied by a displacement along  $c^*$  of the node nearest to the position  $q = 0.1 \text{ \AA}^{-1}$  from  $q = 0.06\text{--}0.07 \text{ \AA}^{-1}$  for  $R = 0$  to  $q = 0.091\text{--}0.095 \text{ \AA}^{-1}$  for  $R = 3$ . In XRD patterns for glycolated I/S, this feature is revealed in the following fashion. A reflection with  $d < 11.9 \text{ \AA}$  will occur on the XRD pattern for I/S with  $R = 3$  and  $w_1 > 0.75$ ; in the case of  $R = 2$  and  $w_1 > 0.67$ , this reflection occurs in the interval  $d = 12.3\text{--}11.9 \text{ \AA}$  which varies with changes in  $w_1$  and turns out to be  $d = 13.5\text{--}12.3 \text{ \AA}$  for  $0.67 > w_1 > 0.5$ . If  $R = 1$  and  $w_1 > w_s$ , the reflection occurs at  $d = 13.5 \text{ \AA}$  and at  $d = 17 \text{ \AA}$  if  $R = 0$  and  $w_s > w_1$ . Note that other low-angle reflections corresponding to  $q < 0.07 \text{ \AA}^{-1}$ , which are expected for I/S with  $R > 1$ , disappear more

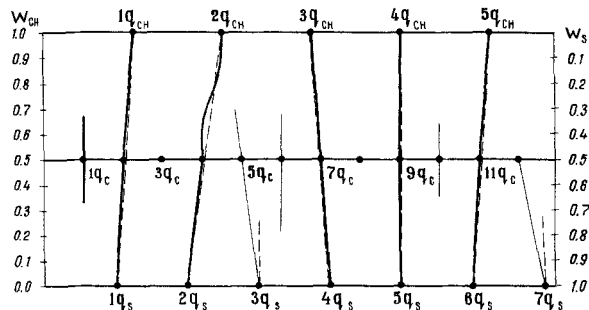


Figure 4. Graphical simulation of node positions along  $c^*$  for glycerol-containing chlorite/smectite (Ch/S) with  $R = 0$  (dashed lines) and  $R = 1$  (solid lines), as a function of layer type proportion. Thin solid lines represent migration nodes with low structure factors. CH = chlorite; C = corrensite; and S = smectite.

rapidly with increasing disorder and illite layer proportion than predicted by rule 1. The diffraction features predicted by this technique are in agreement with those found by Reynolds and Hower (1970) and Drits and Sakharov (1976).

In a similar fashion, the graphical simulation technique can be applied to other interstratified minerals. For example, the rectangle in Figure 4 is a schematic representation of node positions along  $c^*$  to be expected for mixed-layer chlorite-smectite (Ch/S) with  $R = 0$  (dashed lines) and  $R = 1$  (solid lines). In the latter case, the interaction was considered between the corrensite  $00l$  reciprocal lattice nodes with period  $q_c = 1/(17.8 + 14.2) = 1/32 = 0.03125 \text{ \AA}^{-1}$  and the nearest chlorite ( $w_{\text{Ch}} > 0.5$ , the upper part of the rectangle) and smectite ( $w_s > 0.5$ , the lower part of the rectangle)  $00l$  nodes. Again, there are two groups of lines, one representing the migration of nodes depending mostly on  $w_{\text{Ch}}$  and the other representing that of the nodes depending on layer-type distribution. Problems in evaluating  $R$  arise when one of the components dominates, e.g., when  $w_{\text{Ch}} > 0.8$  (Figure 4). Therefore, the peak positions can not be used for the determination of the  $R$  value.

Proportions of component layers can be determined by using the graphical technique or can be calculated with the help of simple linear relationships. As an example of a calculation, let us consider illite-smectite with  $w_1 > w_s$ ,  $R = 1$  and layer thicknesses of illite, smectite and rectorite  $d_1 = 10.0 \text{ \AA}$ ,  $d_s = 16.9 \text{ \AA}$ , and  $d_r = 26.9 \text{ \AA}$  (ethylene glycol), respectively. Figure 5 indicates that, in the interval  $d = 10.0\text{--}8.967 \text{ \AA}$ , the following relationship for determining the proportion of smectite can be easily obtained:

$$w_s = 0.5 \frac{1/d_{\text{obs}} - 1/d_1}{3/d_r - 1/d_1} = \frac{(d_1 - d_{\text{obs}})d_r}{2(3d_1 - d_r)d_{\text{obs}}}$$

$$= 4.339 \frac{10 - d_{\text{obs}}}{d_{\text{obs}}}$$

In a similar way the relationships for the reflections occurring in the intervals  $d = 5.0\text{--}5.38 \text{ \AA}$  and  $d = 2.0\text{--}2.069 \text{ \AA}$  can be obtained:

$$\begin{aligned} w_s &= 0.5 \frac{2/d_1 - 1/d_{\text{obs}}}{2/d_1 - 5/d_r} = \frac{(2d_{\text{obs}} - d_1)d_r}{2(2d_r - 5d_1)d_{\text{obs}}} \\ &= 7.079 \frac{d_{\text{obs}} - 5}{d_{\text{obs}}} \end{aligned}$$

and

$$\begin{aligned} w_s &= 0.5 \frac{5/d_1 - 1/d_{\text{obs}}}{5/d_1 - 13/d_r} = \frac{(5d_{\text{obs}} - d_1)d_r}{2(5d_r - 13d_1)d_{\text{obs}}} \\ &= 14.944 \frac{d_{\text{obs}} - 2}{d_{\text{obs}}}, \end{aligned}$$

respectively. A similar relationship can be derived for any mixed-layer structure with any  $R$  and any layer thickness, but only for those reflections with similar intensities whose positions are insensitive to  $R$ .

#### APPLICATION AND DISCUSSION OF THE TECHNIQUE

The technique was tested on illite-smectites studied in detail and reported in papers by Środón (1980, 1984), Reynolds and Hower (1970), McCarty and Thompson (1991), and Drits and Sakharov (1976). These papers describe illite-smectites with different  $R$  values (from 0 to 3) and different proportions of illite and smectite layers. Structural parameters of illite-smectites were obtained on the basis of a satisfactory agreement between experimental and simulated XRD curves for glycolated samples. Basal  $d$  values reported in these papers were used for determining  $R$  and proportions of illite layers ( $w_1$ ). The illite and smectite layer thicknesses were taken equal to  $10 \text{ \AA}$  and  $16.9 \text{ \AA}$ , respectively. The  $w_1$  values were determined from basal reflections whose  $d$  values occurred in the following intervals;  $10.0\text{--}8.45 \text{ \AA}$ ,  $5.0\text{--}5.63 \text{ \AA}$ , and  $2.00\text{--}2.11 \text{ \AA}$  (Table 1). It should be noted that, for illite-smectites with  $R = 0$ ,  $w_1$  was determined by the technique described for illite-smectites with  $R = 1$ . Comparison between  $R$  and  $w_1$  values reported in the literature and those determined by the technique proposed permits us to conclude that  $R$  values coincide for all illite-smectites, and absolute  $w_1$  values differ by 2%–6%. Therefore, the technique proposed is suitable for fast, simple, and reliable determinations of basic structural parameters of illite-smectites over a wide range of  $R$  and  $w_1$ .

One of the advantages of this technique is the fact that it permits a simple simulation of peak positions for illite-smectites with different thicknesses of illite and smectite layers. Moreover, the exact thickness of the interstratified layers can be determined by the trial and error method. A very spectacular example can be

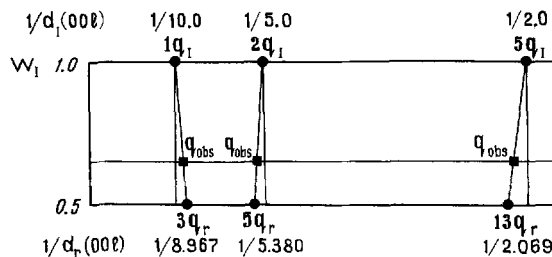


Figure 5. Node positions along  $c^*$  used in linear relationships for calculating the proportion of illite layers in glycolated I/S with  $R = 1$  and  $w_1 > 0.5$ .

demonstrated with XRD curves for illite-smectites reported by Brusewitz (1986). Table 2 shows the  $w_1$  values determined from experimental  $d$  values occurring in the intervals  $5.08\text{--}5.46 \text{ \AA}$  and  $8.884\text{--}9.82 \text{ \AA}$ . Three models of illite-smectite were used with different thicknesses of smectite layers:  $16.7 \text{ \AA}$ ,  $16.9 \text{ \AA}$ , and  $17.0 \text{ \AA}$ , respectively, but with the same thickness of illite layers,  $10 \text{ \AA}$ . Table 2 indicates that only when  $d_s = 17.0 \text{ \AA}$  do  $w_1$  values determined from two experimental  $d$ -values lie close to each other, whereas only the average  $w_1$  values determined for each given smectite layer thickness are similar.

The results obtained with the proposed technique coincide quite well in the case of illite-smectites, but proportions of interstratified layers in other mixed-layer systems such as kaolinite-smectite, chlorite-smectite, and biotite-vermiculite can only be estimated with lower accuracy. This can be explained by the greater (than for illite-smectites) difference in the values of the structure factors of basal reflections in periodic structures of pure components whose “interaction” controls the shift of the basal reflections for the mixed-layer mineral. Also there are only a few publications reporting experimental and calculated XRD patterns for these minerals. For these minerals, most investigators use the tables proposed by Moore and Reynolds (1989) and by Drits and Sakharov (1976) where  $d$  values determined from simulated XRD curves are given for various minerals with  $R = 0$ ,  $R = 1$ , and various proportions of interstratified components.

Table 3 compares the proportion of kaolinite, chlorite, or biotite layers in mixed-layer kaolinite-smectite, chlorite-smectite, and biotite-vermiculite determined with the help of the technique proposed. The  $d$  values for basal reflections occurring on the simulated XRD curves at certain contents (10%, 20%, 30%, etc.) of corresponding layers were used as initial data. These  $d$  values were used for determining the proportion of layers. They are given in the papers referred to in Table 3, while the table itself gives only the intervals containing them. As in the case of I/S, proportions of layers were determined assuming  $R = 1$  even though the interstratification was of the type  $R = 0$ .

Table 1. Comparison between the R (Reichweite) and the percentage of illite layers in illite-smectites, as determined by the graphical technique and reported in literature.

Identification	Sample parameters <sup>1</sup>		Parameters determined by the proposed technique	
	R	Wl%	R	Wl% <sup>2</sup>
Sample 1	R1	51	R1	48
2	R1	52	R1	48
3	R1	52	R1	52
4	R1	56	R1	54
5	R1	61	R1	61
6	R1	63	R1	61
7	R1	62	R1	61
8	R1	64	R1	60
9	R1	62	R1	67
10	R1	68	R1	66
11	R1	68	R1	66
12	R1	71	R1	71
13	R1	72	R1	69
14	R1	75	R1	76
15	R1/R3	80	R2	78
16	R1/R3	80	R2	79
17	R3	83	R3	82
18	R1/R3	85	R2	90
19	R1/R3	87	R3	89
20	R3	91	R3	92
21	R3	91	R3	92
23	R3	93	R3	95
24	R3	94	R3	95
Sample 6565	R1	58	R1	55
7576	R1	60	R1	58
7590	R1	65	R1	63
7889	R3	80	R3	80
7895	R1.5	74	R2	72
7920	R3	88	R3	88
7958	R3	82	R3	83
7958a	R1	70	R1	65
Kinneulle A-2	R1	68	R1	68
Two Medicine	R1	65	R1	64
Kinneulle B-1	R0	40	R0	43
Kalkberg	R3	90	R3	91
Sample D-17	R1	70	R1	67
D-18	R1	68	R1	67
D-20	R1	76	R1	75
D-25	R2	67	R2	67
D-29	R2	78	R2	80
D-30	R2	80	R2	83
D-35	R3	87	R3	90
D-26	R3	84	R3	85
Sample Sr-2M9	R0	12	R0	12
Sr-2M3	R0	20	R0	16
Sr-4M2	R0	22	R0	20
Na-2R50	R0	37	R0	33
Na-2R49	R1	52	R1	50
Sr-1M6	R1	59	R1	54
Sr-Ch5	R1	63	R1	60
Na-2R63	R1	68	R1	66
Sr-2R62	R1	71	R1	67
Na-T9	R1	80	R1	77
K-2R76	R0	58	R0	56
Ca-2R76	R0	44	R0	45
Arkansas	R1	52	R1	55
Zempleni	R3	82	R3	81
XIII	R0	7	R0	10

<sup>1</sup> Samples 1–24, Środoń (1984); samples 6565–7958 (calculated diffraction patterns), McCarty and Thompson (1991); Kinneulle, Two Medicine, Kalkberg, Reynolds and Hower

Table 2. The effect of smectite layer thickness,  $d_s$ , on the proportion of illite,  $w_i$  %, in mixed-layer illite-smectite.

Sample <sup>1</sup>	$w_i$ % <sup>1</sup>	$d_s$ , Å	$w_i$ %		
			$d_s = 16.7$ Å	$d_s = 16.9$ Å	$d_s = 17.0$ Å
B-39	46	5.46 8.84	23 43	33 40	39 35
B-37	51	5.41 8.95	av. 33 51	av. 37 51	av. 37 46
B-36	54	5.40 9.03	av. 42 56	av. 46 55	av. 47 52
B-34	56	5.38 9.12	av. 45 42	av. 50 50	av. 51 52
B-32	62	5.36 9.21	av. 51 60	av. 55 60	av. 54 56
K-15	90	5.08 9.82	av. 55 88	av. 58 91	av. 58 91
K-74	70	5.31 9.26	av. 90 55	av. 92 58	av. 92 61
			av. 60	av. 62	av. 62

<sup>1</sup> Data from Brusewitz (1986).

Table 3 indicates that agreement between proportions of kaolinite layers in kaolinite-smectite with  $R = 0$  can be obtained by using the reflection occurring in the interval  $d = 7.15$ – $8.45$  Å (glycolated complex) and  $d = 7.15$ – $8.89$  Å (complex with glycerol). But disagreement between true and calculated  $w_k$  values was obtained for the basal reflection occurring in the interval  $d = 3.380$ – $3.575$  Å.

Proportions of chlorite layers,  $w_{ch}$ , in chlorite-smectite structures with  $R = 0$  (glycolated complex) can be determined by using two reflections whose  $d$  values lie in the intervals:  $d = 7.15$ – $8.45$  Å and  $d = 3.380$ – $3.575$  Å, and taking an average value of  $w_{ch}$ . The  $d$  values occurring in the interval  $3.33$ – $3.57$  Å lead to agreement between actual and estimated proportions of layer types for biotite-vermiculite structures with  $R = 0$  and  $R = 1$ .

## CONCLUSIONS

The main advantage of the technique described is that it is a very simple simulation of basal peak positions for two-component mixed-layer structures with different R values and different layer thicknesses. For I/S, R and  $w_i$  values determined for the glycolated and glycerol complexes agree quite well with actual R val-

(1970); samples D-17–D-36, Drits and Sakharov (1976, Table 13, p. 168); the others, Środoń (1980).

<sup>2</sup> Average of three reflections occurring in the following  $d$ -intervals:  $8.45$ – $10.0$  Å,  $5.0$ – $5.63$  Å, and  $2.00$ – $2.11$  Å.

Table 3. The percentage of kaolinite, chlorite, or biotite in two-component mixed-layer systems, as determined by the technique and used for calculations of corresponding XRD patterns.

Mixed-layer system	R	Intervals of d where useful reflections occur, Å										Reference
		10	20	30	40	50	60	70	80	90		
Observed percentages <sup>2</sup>												
<b>Kaolinite-smectite</b>												
$d_{k,001} = 7.15 \text{ \AA}$	R0	10	20	29	38	51	58	65	76	90	Moore and Reynolds (1989)	
Saturated with ethylene glycol												
$d_{s,001} = 16.90 \text{ \AA}$	R0	10	10	20	29	45	51	61	72	85		
Saturated with glycerol												
$d_{s,001} = 17.78 \text{ \AA}$	R0	7	19	25	38	53	58	68	83	96	Drits and Sakharov (1976)	
	R1	—	—	25	40	—	55	63	76	—		
Heated $d_{s,001} = 9.60 \text{ \AA}$	R0	5	13	24	35	50	61	74	84	92	Drits and Sakharov (1976)	
	R1	—	—	27	40	—	55	64	79	—	Drits and Sakharov (1976)	
		—	—	31	43	—	58	68	76	—		
<b>Chlorite-smectite</b>												
$d_{r,001} = 14.2 \text{ \AA}$	R0	9	17	26	35	48	65	78	86	96	Reynolds (1988)	
$d_{s,001} = 17.0 \text{ \AA}$		8	16	30	37	44	58	72	86	92		
<b>Biotite-vermiculite</b>												
$d_{b,001} = 10.0 \text{ \AA}$	R0	8	15	—	38	50	60	71	77	78	Moore and Reynolds (1989)	
$d_{r,001} = 14.4 \text{ \AA}$		17	22	33	45	50	58	67	76	88	Reynolds (1988)	
$d_{b,001} = 10.05 \text{ \AA}$	R1	—	—	—	—	—	—	—	—	—		
$d_{r,001} = 14.3 \text{ \AA}$		—	—	—	—	—	—	—	—	—		

<sup>1</sup> The percentage of layer types used for calculating XRD patterns for the mixed-layer systems in the corresponding papers.

<sup>2</sup> The percentage estimated by the technique proposed from d values of basal reflections in the calculated XRD patterns.



ues and proportions of illite and smectite layers. For chlorite-smectites, kaolinite-smectites and biotite-vermiculites semiquantitative data can be easily obtained if reflections are used that are situated between nearest reciprocal lattice nodes of periodic components having similar structural amplitudes. Reflection positions for the mixed-layer structures in question are indicated in Table 3. Proportions of component layers in a mixed-layer structure can also be determined from simple linear relationships when R and layer thicknesses are known.

To conclude, note that the technique suggested becomes inefficient for determination of the proportion of layer types if the reciprocal lattice nodes for different components are of substantially different structural amplitudes and do not form pairs at short distances along  $c^*$ . In the region of very low  $2\theta$  angles corresponding to  $q < 0.06\text{--}0.07 \text{ \AA}^{-1}$  considerable deviations from rule 1 are observed, since the resolution of reflections decreases rapidly with decreasing  $q$ . Finally, one should not expect the simulated  $q = 1/d$  values to coincide with the experimental values for reflections sensitive to order/disorder. To determine R, it is sufficient that the  $q_{\text{obs}}$  values for these reflections be, for the given  $w_i$ , close to the positions along  $c^*$  for nodes sensitive to order/disorder for the given R.

## REFERENCES

- Brusewitz, A. M. (1986) Chemical and physical properties of Paleozoic potassium bentonites from Kinnekulle, Sweden: *Clays & Clay Minerals* **34**, 442–454.
- Drits, V. A. and Sakharov, B. A. (1976) *X-ray Structural Analysis of Mixed-Layer Minerals*: Academy of Science, U.S.S.R., 256 pp. (in Russian).
- McCarty, D. K. and Thompson, G. R. (1991) Burial diagenesis in two Montana Tertiary basins: *Clays & Clay Minerals* **39**, 293–305.
- Méring, J. (1949) L'interférence des rayons-X dans les systèmes à stratification désordonnée: *Acta Crystallogr.* **3**, 371–377.
- Moore, D. M. and Reynolds Jr., R. C., (1989) *X-ray Diffraction and the Identification and Analysis of Clay Minerals*: Oxford University Press, 332 pp.
- Reynolds Jr., R. C. (1988) Mixed layer chlorite minerals: in *Hydrous Phyllosilicates (Exclusive of Micas)*, vol. 19, S. W. Bailey, ed., Mineralogical Society of America, Chelsea, Michigan, 725 pp.
- Reynolds Jr., R. C. and Hower, J. (1970) The nature of interlayering in mixed-layer illite-montmorillonites: *Clays & Clay Minerals* **18**, 25–36.
- Šrodón, J. (1980) Precise identification of illite/smectite interstratifications by X-ray powder diffraction: *Clays & Clay Minerals* **28**, 401–411.
- Šrodón, J. (1984) X-ray powder diffraction identification of illitic materials: *Clays & Clay Minerals* **32**, 337–349.

(Received 11 January 1993; accepted 1 February 1994; Ms. 2304)